J|A|C|S
ARTICLES
Published on Web 05/31/2002

The Solute−Solvent System: Solvent Constraints on the Conformational Dynamics of Acetylcholine

Giulio Vistoli,[†] Alessandro Pedretti,[†] Luigi Villa,[†] and Bernard Testa*[,‡]

Contribution from the Istituto di Chimica Farmaceutica, Facoltà di Farmacia, Università di Milano, Viale Abruzzi 42, I-20131 Milano, Italy, and Institut de Chimie thérapeutique, Section de pharmacie, Université de Lausanne, CH-1015 Lausanne-Dorigny, Switzerland

Received August 20, 2001. Revised Manuscript Received January 24, 2002

Abstract: The objective of this study was to determine if and how a solvent influences internal motions in a solute molecule. Acetylcholine was chosen as the object of study given its interesting molecular structure and major biological significance. Molecular dynamics simulations were carried out in the vacuum (10 ns), water (5 ns), methanol (5 ns), and octanol (1.5 ns). Seven clusters of conformers were identified, namely, +g+g, −g−g, +gt, −gt, t+g, t−g, and tt, where the gauche and trans labels refer to the dihedral angles τ_2 and τ_3, respectively. As expected, the relative proportion of these conformational clusters was highly solvent-dependent and corresponded to a progressive loss of conformational freedom with increasing molecular weight of the solvent. More importantly, the conformational clusters were used to calculate instantaneous and median angular velocity (ω and ω_M, respectively) and instantaneous and median angular acceleration (α and α_M, respectively). Angular velocity and angular acceleration were both found to decrease markedly with increasing molecular weight of the solvent, i.e., vacuum ($\epsilon = 1$) > water > methanol > octanol. The decrease from the vacuum to octanol was ∼40% for τ_2 and ∼60% for τ_3. Such solvent-dependent constraints on a solute's internal motions may be biologically and pharmacologically relevant.

Introduction

One of the most fundamental quests in chemistry is to constantly deepen our understanding of molecular structure taken in its broadest sense, namely, its geometry and physicochemical properties. In particular, significant changes are seen when molecular properties are investigated in vacuum or in solution, using experimental and computational methods of investigations.[1−4] For example, a solvent can influence the electronic properties of the solute, which will exhibit changes in its color and UV spectrum. Similarly, and as a rule, the conformational behavior of a solute is strongly affected by the solvent.

Such an effect is double, affecting both the relative stability of conformers and the dynamics of intramolecular motions. But while solvent-dependent conformational equilibria have been extensively investigated, medium-dependent constraints on intramolecular motions remain a poorly explored field. Yet such constraints should not be without influence on the behavior of compounds in biological systems, e.g., when they permeate membranes or bind to biological targets such as enzymes and receptors.

The present study offers an approach to solvent-dependent constraints on conformational dynamics (i.e., rates of conformational motions). Acetylcholine was chosen as the object of study given its interesting molecular structure, major biological significance, and the many data (experimental and computational) accumulated on its conformational behavior.[5−19] Molecular dynamics (MD) simulations were used to compare the rates of conformational motions (median angular velocity and acceleration) of acetylcholine in the vacuum ($\epsilon = 1$ and 80) and in three solvents of decreasing polarity, i.e., water, methanol, and octanol. Very few comparable studies exist; for example, the conformation of NAD^+ was simulated in various environ-

* To whom correspondence should be addressed. Phone: +41 21 692 4521. Fax: +41 21 692 4525. E-mail: Bernard.Testa@ict.unil.ch.
[†] Università di Milano.
[‡] Université de Lausanne.

(1) Testa, B.; Kier, L. B.; Carrupt, P. A. *Med. Res. Rev.* **1997**, *17*, 303−326.
(2) Testa, B.; Bojarski, A. J. *Eur. J. Pharm. Sci.* **2000**, *11* (Suppl. 2), S3−S14.
(3) Rabitz, H. *Science* **1989**, *246*, 221−226.
(4) Testa, B.; Kier, L. B. *Entropy* **2000**, *2*, 1−25. http://www.mdpi.org/entropy/papers/e2010001.pdf
(5) Chothia, C.; Pauling, P. J. *Nature* **1969**, *223*, 919−21.
(6) Partington, P.; Feeney, J.; Burgen, A. S. V. *Mol. Pharmacol.* **1972**, *8*, 269−277.
(7) Pullman, B.; Courrière, P. *Mol. Pharmacol.* **1972**, *8*, 612−622.
(8) Genson, D. W.; Christoffersen, R. E. *J. Am. Chem. Soc.* **1973**, *95*, 362−368.
(9) Radna, R. J.; Beveridge, D. L.; Bender, A. L. *J. Am. Chem. Soc.* **1973**, *95*, 3831−3842.
(10) Beveridge, D. L.; Kelly, M. M.; Radna, R. J. *J. Am. Chem. Soc.* **1974**, *96*, 3769−3778.
(11) Gelin, B. R.; Karplus, M. *J. Am. Chem. Soc.* **1975**, *97*, 6996−7006.
(12) Langlet, J.; Claverie, P.; Pullman, B.; Piazzola, D.; Daudey, J. P. *Theor. Chim. Acta* **1977**, *46*, 105−116.
(13) Margheritis, C.; Corongiu, G. *J. Comput. Chem.* **1988**, *9*, 1−10.
(14) Behling, R. W.; Yamane, T.; Navon, G.; Jelinsky, L. W. *Proc. Natl. Acad. Sci. U.S.A.* **1988**, *85*, 6721−6725.
(15) Kim, Y. J.; Kim, S. C.; Kang, Y. K. *J. Mol. Struct.* **1992**, *269*, 231−241.
(16) Segall, M. D.; Payne, M. C.; Boyes, R. N. *Mol. Phys.* **1998**, *93*, 365−370.
(17) Deakyne, C. A.; Meot-Ner, M. *J. Am. Chem. Soc.* **1999**, *121*, 1546−1557.
(18) Williamson, P. T. F.; Watts, J. A.; Addona, G. H.; Miller, K. W.; Watts, A. *Proc. Natl. Acad. Sci. U.S.A.* **2001**, *98*, 2346−2351.
(19) Marino, T.; Russo, N.; Toci, E.; Toscano, M. *Theor. Chem. Acc.* **2001**, *107*, 8−14.

10.1021/ja0119999 CCC: $22.00

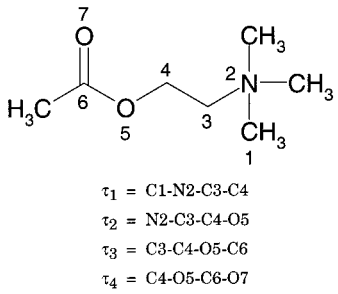

Figure 1. Dihedral angles in acetylcholine. Their values in this study are defined according to Klyne and Prelog.[21]

ments for 5 ns, but the study was focused on conformational preference and intramolecular interactions.[20] The results of the present study demonstrate and assess the constraints imposed by the solvent on the dynamics of internal motions.

Methods

Systematic Conformational Analysis. The initial geometry of acetylcholine was constructed and was energy-minimized using the Quanta/CHARMm package (MSI, Burlington, MA). The computation of partial atomic charges and the final geometry optimization were carried out at the semiempirical level with the MOPAC6.0 program (www.ccl.net), keywords = AM1, PRECISE, GEO-OK.

The conformational profile of acetylcholine in the vacuum ($\epsilon = 1$) was first examined by a systematic conformational analysis using Quanta/CHARMm. The torsion angles τ_2 and τ_3 (Figure 1) were rotated by increments of 10°, yielding $36 \times 36 = 1296$ conformers. The structures obtained during this systematic search was minimized, and the geometry of the minimum-energy conformers so identified was optimized using MOPAC6.0.

Molecular Dynamics Simulations. All calculations were carried out in an SGI Indigo^2 R4400 workstation. The package Quanta/CHARMm with the force field CHARMm v22 (1992) was used. The initial structure of acetylcholine for all simulations is the +g+g geometry (i.e., in which τ_2 and τ_3 are gauche) obtained from the above systematic analysis. This structure was submitted to molecular dynamics simulations of various durations (10 ns for acetylcholine at $\epsilon = 1$; 5 ns at $\epsilon = 80$, in water and in methanol; 1.5 ns in octanol). No constraint was imposed on any of the dihedral angles; except when indicated otherwise only τ_2 and τ_3 were monitored.

The choice of the initial conformation might be suspected to influence the results of a simulation. For this reason, we used a prolonged duration of equilibration (400 ps) which renders negligible the risk of biased results for the simulations in vacuum. However, this risk may no longer be negligible for simulations in water and in methanol. We therefore carried out two short simulations (2 ns) in water and in methanol, starting from the tt conformer and found that except for a short initial period the results were similar to those obtained when starting with a gg conformer. As far as the simulation in octanol is concerned, the results are indeed markedly influenced by the starting conformer, as discussed later.

For the simulations in water and methanol, the starting structure of acetylcholine was placed in a cluster of radius 10 Å containing 164 water molecules described by the model TIP3S or 94 methanol molecules described by the appropriate template in Quanta/CHARMm.

The cluster of hydrated octanol was constructed as follows: (1) construction of the molecules of 1-octanol in its favored, zigzag conformation, energy minimization by Quanta/CHARMm, optimization, and calculation of partial charges using MOPAC6.0; (2) construction of the complex made of one water and four octanol molecules, energy minimization of the complex using Quanta/CHARMm, optimization, and calculation of partial charges using MOPAC6.0; (3) building of a solvent cluster with the following dimensions, four complex units in the *X* axis, two in the *Y* axis, and three in the *Z* axis, i.e., a total of 96 octanol molecules and 24 water molecules; (4) insertion of the cluster in a box with periodic boundary conditions (PBC) and orthogonal axes of dimensions $X = 30$ Å, $Y = 40$ Å, and $Z = 20$ Å.

All solvent clusters (water, methanol, hydrated octanol) were then optimized for the relative position of the solvent molecules, to eliminate any high-energy interaction. The molecular dynamics simulations of acetylcholine were carried out for 5 ns in water and methanol and 1.5 ns in octanol.

All simulations had the following characteristics: minimizations with the conjugate gradients algorithm, convergence limit (rms) 0.01, maximal number of iterations 5000; molecular dynamics with constant temperature in the range 300 ± 25 K, integration of Newton's equation each 1 fs according to Verlet's algorithm, calculation of initial atomic velocities according to Boltzmann's equation, and frame stored each 1000 iterations (1.0 ps). The molecular dynamics were carried out in three phases: initial period of heating from 0 to 300 K over 3000 iterations (3 ps, i.e., 1 K/10 iterations), equilibration period 400 ps with recalculation of atomic velocities during this period each 0.2 ps, and the monitored phase of simulation of 10, 5, or 1.5 ns as indicated. Only the frames memorized during this third phase were considered in the conformational analyses.

The results of the MD simulations were analyzed with Fortran programs especially written for the task using the Software Development Kit in the Irix6.2 system.

Rates and Accelerations of Interconversion. The rates of conformational interconversion were analyzed in terms of *instantaneous* and *median angular velocity* (ω and ω_M, respectively) and of *instantaneous* and *median angular acceleration* (α and α_M, respectively). Having a given dihedral angle τ in two consecutive frames (τ_i and τ_{i+1}), one can calculate the instantaneous angular velocity (ω_i) as per eq 1, where *t* is

$$\omega_i = \frac{\Delta\tau}{t} = \frac{|\tau_{i+1} - \tau_i|}{t} \tag{1}$$

the time interval between two frames (here 0.5 ps). From such values, one can then calculate a median angular velocity for *N* frames (eq 2):

$$\omega_M = \sum \omega_i/(N-1) \tag{2}$$

Similarly, an instantaneous angular acceleration (α_i) was calculated as the difference between two consecutive instantaneous velocities (ω_i and ω_{i+1}) (eq 3). Median angular accelerations were obtained according to eq 4:

$$\alpha_i = \frac{\Delta\omega}{t} = \frac{|\omega_{i+1} - \omega_i|}{t} \tag{3}$$

$$\alpha_M = \sum \alpha_i/(N-2) \tag{4}$$

Results

Systematic Conformational Analysis of Acetylcholine in Vacuum. Acetylcholine has four dihedral angles defined in Figure 1. Preliminary calculations confirmed literature data, indicating that τ_1 and τ_4 vary in a narrow range and independently of the conditions ($\tau_1 = 60° \pm 20°$; and $\tau_4 = 0° \pm 20°$), due to the symmetry of the triple rotor τ_1 and to the rigidity of the ester group (τ_4).[21] This allowed us to keep constant $\tau_1 = 60°$ and $\tau_4 = 0°$ (carbonyl oxygen eclipsing C4) and to focus on the dihedral angles τ_2 and τ_3, which describe most of the conformational behavior of acetylcholine.

(20) Smith, P. E.; Tanner, J. J. *J. Mol. Recognit.* **2000**, *13*, 27−34.

(21) Klyne, W.; Prelog, V. *Experientia* **1960**, *17*, 521−523.

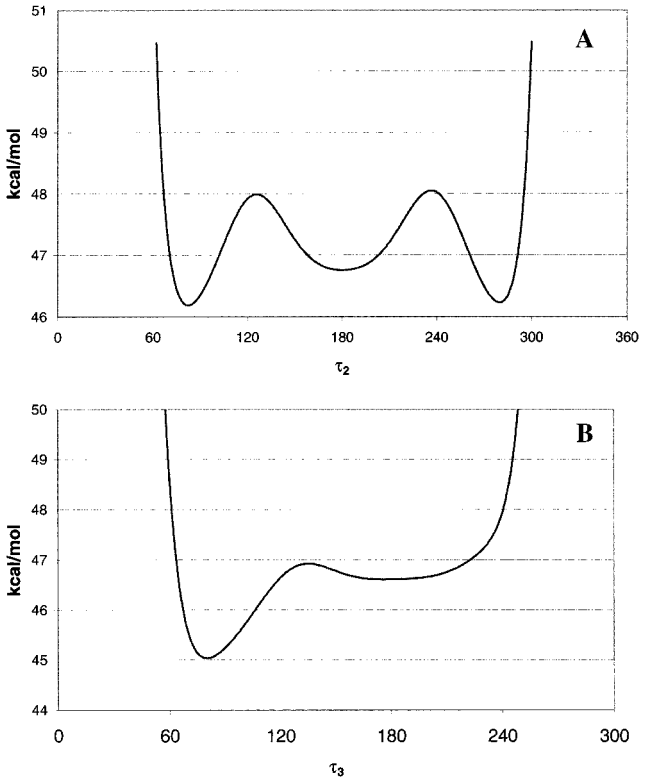

Figure 2. Variations of the dihedral angles of acetylcholine in vacuum ($\epsilon = 1$; temperature, 300 K). Note that the dihedral angles are taken to vary from 0° to 360°. (A) τ_2; (B) τ_3, with $\tau_2 = +g$.

Table 1. Classification of Dihedral Angles[21]

range of τ (deg)	designation	symbol
$\tau > 330$ or $\tau < 30$	syn-periplanar	0
$30 < \tau < 90$	(+)-syn-clinal or (+)-gauche	+g
$90 < \tau < 150$	(+)-anti-clinal	+a
$150 < \tau < 210$	anti-periplanar or trans	t
$210 < \tau < 270$	(−)-anti-clinal	−a
$270 < \tau < 330$	(−)-syn-clinal or (−)-gauche	−g

The conformational profile of acetylcholine in the vacuum with $\epsilon = 1$ was first examined by a systematic conformational analysis, and the various angular values were grouped in six classes as defined in Table 1. The conformational behavior of acetylcholine around dihedral angles τ_2 and τ_3 is presented in Figure 2A and B, respectively. Except in the syn-periplanar conformation, the dihedral angle τ_2 proved independent of the value of τ_3 and showed two symmetric global minimums at ∼+80° (+g) and ∼+280° (−g) and a local minimum (at +0.5 kcal/mol) around 180° (t). The energy barrier between the two global minimums is close to +2 kcal/mol (+a and −a). In contrast, the syn-periplanar conformation is highly improbable (e.g., +220 kcal/mol when τ_3 is trans). Thus the path of conformational flexibility for τ_2 is essentially

$$+g \leftrightarrows +a \leftrightarrows t \leftrightarrows -a \leftrightarrows -g$$

As for the dihedral angle τ_3 (Figure 2B), its energy profile markedly depends on τ_2. When τ_2 is trans, the profile of τ_3 is similar to that of τ_2 in Figure 2A (not shown), with the trans conformation ∼+1.2 kcal/mol above the +g and −g global minimums. In contrast, when τ_2 is +g, the energy profile of τ_3 is dissymmetric (Figure 2B) and shows only one global minimum (+g), a broad local minimum (t and −a) at ∼+1.6 to +1.8 kcal/mol), and a barrier (+a) at ∼+2 kcal/mol. Again, the syn-periplanar conformation is highly improbable (e.g., +50 kcal/mol) when τ_2 is trans. In addition, $\tau_3 = -g$ is also too energetic when τ_2 is +g (Figure 2B). When τ_2 is −g, the energy profile of τ_3 is the mirror image of that shown in Figure 2B, with $\tau_3 = -g$ as the global minimum and $\tau_3 = +g$ as a highly improbable conformer. In other words, the path of conformational flexibility for τ_3 is essentially

$$+g \leftrightarrows +a \leftrightarrows t \leftrightarrows -a \quad \text{when} \quad \tau_2 = +g$$

and

$$+a \leftrightarrows t \leftrightarrows -a \leftrightarrows -g \quad \text{when} \quad \tau_2 = -g$$

These conformational profiles define 11 minimum-energy conformations, and 13 transition conformations, as presented in Table 2. The other possibilities in Table 2 correspond to highly improbable conformations and are left blank. The geometry of the 11 minimum-energy conformers was optimized using Quanta/CHARMm followed by MOPAC6.0. Interestingly, the minimums +g+g and +g+a converged to the same +g+g conformer, indicating that they correspond to a single conformational cluster. The same was true for +gt and +g−a, which converged to +gt, for −g+a and −gt, which converged to −gt, and for −g−a and −g−g, which converged to −g−g.

The optimized geometry and relative energy of the seven resulting conformers are summarized in Table 3 and displayed in Figure 3. Remarquably, three pairs of conformers are apparent (+g+g and −g−g, +gt and −gt, t+g and t−g), whose relative energies are similar and whose angular values are mirror images. In these six conformers, stabilization appears due, at least in part, to favorable electrostatic interactions between an electron-poor methyl group in the cationic head and the oxygen atoms. In contrast, the conformer tt has unique characteristics and a higher relative energy.

Our results are in good correspondence with those obtained by Segall et al. using ab initio methods based on density functional theory.[16] Indeed, this study revealed that the angles τ_2 and τ_3 can exist in the gauche and trans ranges, with an energy minimum for the −gt conformer and the tt conformer being possible only in relaxed molecular structures. Even the energy difference between the −gt and tt conformers obtained here by simple molecular mecanical calculations is in good agreement with the ab initio results (ΔE ∼6 kcal/mol with the two methods).

In summary, this preliminary exploration has identified preferred conformers and preferred transitions of acetylcholine. The goal here was more qualitative than quantitative and served to lay the ground for the real objectives of this study, which were to explore the influence of the medium on the conformational profile of acetylcholine and mainly on its rates of dihedral rotations. In the molecular dynamics to be presented below, the conformational behavior of acetylcholine was monitored under a variety of conditions (in the vacuum at $\epsilon = 1$ and $\epsilon = 80$, in water, in methanol, and in octanol). Populations of conformers were sampled over long durations and essentially confirmed the above results, whereas rates of rotations have been shown to be markedly medium-dependent.

Table 2. Various Conformers of Acetylcholine, Designated as Combinations of τ_2 and τ_3[a]

	τ_2 (range, deg)					
τ_3 (range, deg)	0 (330–30)	+g (30–90)	+a (90–150)	t (150–210)	–a (210–270)	–g (270–330)
0 (330−30)				(t0)		
+g (30−90)		+g+g	(+a+g)	t+g	(−a+g)	
+a (90−150)		+g+a	(+a+a)	(t+a)	(−a+a)	−g+a
t (150−210)		+gt	(+at)	tt	(−at)	−gt
−a (210−270)		+g−a	(+a−a)	(t−a)	(−a−a)	−g−a
−g (270−330)			(+a−g)	t−g	(−a−g)	−g−g

[a] Combinations *not* in parentheses designate the most probable conformers (energy minimums), combinations in parentheses designate conformers of slightly higher energy (transitional conformers), whereas empty boxes correspond to highly improbable conformers.

Table 3. Optimized Properties of the Seven Minimum-Energy Conformers of Acetylcholine Identified by Molecular Dynamics (Vacuum, $\epsilon = 1$)

conformer	τ_2	τ_3	ΔE (kcal/mol)
+g+g	60.9	79.1	+1.94
+gt	68.8	238.9	+0.07
t+g	187.3	80.1	+2.90
tt	180.2	184.3	+6.31
t−g	178.3	299.9	+2.99
−gt	291.6	121.3	0.0
−g−g	299.6	281.7	+1.93

Dynamic Behavior of Acetylcholine in Vacuum at $\epsilon = 1$. The dynamics of acetylcholine in vacuum was simulated for 10 ns, during which 10 000 frames were stored. The trajectories of all four dihedral angles of acetylcholine were monitored and are shown in Figure 4. It can be seen that the angles τ_1 and τ_4 remain practically fixed, with $\tau_1 = 60° \pm 20°$ (Figure 4A) and $\tau_4 = 0° \pm 20°$ (Figure 4D) during the entire simulation.

The angle τ_2 (Figure 4B) is seen to vary in the range +1080° to −360°, with a clear predominance of gauche values and a rare occupation of trans values. The angle τ_3 (Figure 4C) varies even more broadly, from +1440° to −1440° and oscillates between the five possible geometries (+g, −g, and t when τ_2 is trans; +a and −a when τ_2 is gauche). This is due to a somewhat smaller rotational freedom of τ_2 compared to τ_3 due to the steric bulk of the ammonium head. There are also two approximate cycles of 5 ns visible in Figure 4C and D, the first more clearly marked than the second. A count of conformers (Table 4) demonstrates this quite convincingly. Also noteworthy is the fact that for most of the time τ_2 and τ_3 share the same direction of rotation and that this direction is more often positive during the first period of 5 ns, and more often negative during the second period of 5 ns. Indeed, during the first 5 ns, τ_2 is +g about twice as often as it is −g; the opposite is true during the second period of 5 ns.

The resulting conformational distribution in a τ_2 versus τ_3 plot is shown in Figure 5. A symmetric distribution centered on the tt conformers is apparent, with a vast majority of conformers in the classes +g+g, +gt, +g−a, −g+a, −gt, and −g−g and a minority in the classes +g+a, t+g, t−g, and −g−a. The empty regions are the syn-periplanar (0) and anti-clinal (+a and −a) ones for τ_2 and the syn-periplanar (0) ones for τ_3. These results are in excellent agreement with the conformational energies shown in Figure 2A and B.

The median angular velocity ω_M and the median angular acceleration α_M of τ_2 and τ_3 are reported in Tables 5 and 6, respectively. It appears that ω_M and α_M of both angles have comparatively lower values for conformers with τ_2 = gauche and higher values when τ_2 = trans. A symmetry is also apparent such that ω_M and α_M are comparable within the pairs +gt and −gt, +g+g and −g−g, and t+g and t−g.

Dynamic Behavior of Acetylcholine in Vacuum at $\epsilon = 80$. Although such conditions may be devoid of physical meaning, simulations were carried out in vacuum with $\epsilon = 80$ to unravel intramolecular electrostatic effects in the absence of solvent. The simulations were restricted to 5 ns. The angle τ_2 varied in the range +180° to +1080°, with a clear predominance of trans values and less occupation of gauche values, as noted above. The angle τ_3 varied very broadly indeed, between about +3900° to −1700°, oscillating between the five possible geometries (+g, −g, +a, t, −a) with little preference for any of them. This is due to the greater freedom of rotation of τ_3. Also, the harmonic rotation of τ_2 and τ_3 seen at $\epsilon = 1$ was lost at $\epsilon = 80$. Indeed, τ_2 showed constantly positive angles, resulting from a mainly clockwise rotation, whereas τ_3 moves freely clockwise and counterclockwise (results not shown).

The distribution of geometries (τ_2 versus τ_3, Figure 6) shows that the behavior of τ_2 is quite different from that at $\epsilon = 1$ (Figure 5), since the trans conformations predominate over the −g and even more over the +g ones. The predominant conformers have shifted from +g+g, +gt, −g+g, and −gt at $\epsilon = 1$ to t+g, t+a, tt, t−a, and t−g at $\epsilon = 80$. In addition, the distribution of conformers at $\epsilon = 80$ presents a marked dissymmetry, with about twice more τ_2 = −g than +g.

The median angular velocity ω_M and the median angular acceleration α_M of τ_2 and τ_3 are reported in Tables 5 and 6. It appears that the ω_M and α_M values of τ_2 are more uniform than at $\epsilon = 1$, whereas the corresponding values for τ_3 are distinctly higher.

Dynamic Behavior of Acetylcholine in Water. The trajectory of τ_2 and τ_3 in water (Figure 7A and B, respectively) is in marked contrast to the trajectories observed in the vacuum at $\epsilon = 1$ (Figure 4B and C, respectively) and $\epsilon = 80$. The angle τ_2 is seen to reside mainly in syn-clinal (+g and −g) geometries, whereas the trans geometries are fewer and occupied only during 0.5 ns in the period 2.5−3.0 ns. The angle τ_3 shows a continuous distribution of values in the range 60°−300°. with a predominance of anti-periplanar and anti-clinal (+a, t, −a) geometries. A further difference between the two angles is that only τ_2 can undertake full rotations, and this almost exclusively clockwise, whereas τ_3 remains confined in a single phase and never equals 0°. And when the trajectories in vacuum and in water are compared, it is seen that solvent effects are stronger for τ_3 than for τ_2. The proximity of the ester group hydrated via H-bonds is believed to account for this stronger influence. The same effect accounts for the predominance of anti-periplanar and anti-clinal geometries, which render the ester group more accessible to water.

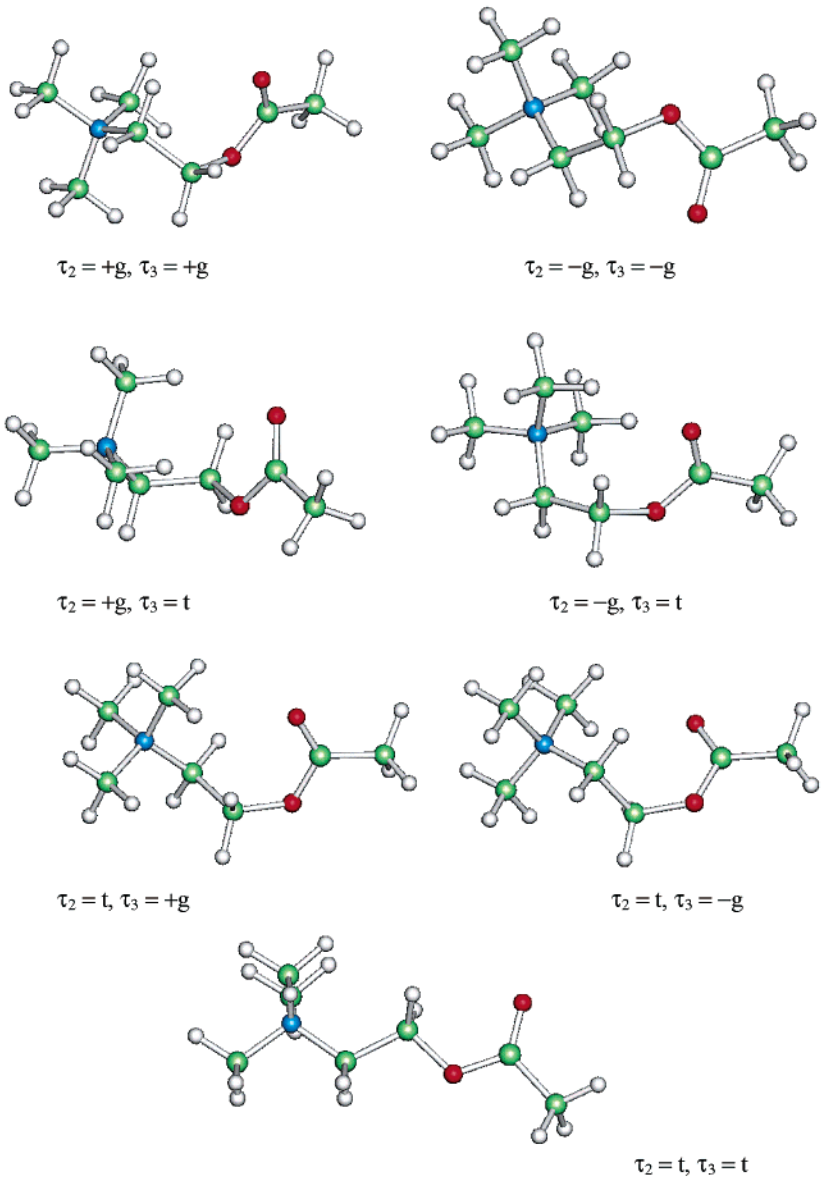

Figure 3. The seven low-energy conformers of acetylcholine characterized here.

Despite the large influence of environment on trajectories notes above, populations of conformers of acetylcholine in water do not vary dramatically relative to the vacuum at $\epsilon = 1$ (Figure 5), resulting in a marked predominance of conformers in the classes +g+g, +gt, +g−a, −g+a, −gt, and −g−g (Figure 8). A marked predominance of $\tau_2 = -g$ is apparent, and the ratio of −g−g over +g+g is close to 2/1. In contrast, +gt and −gt are almost equally distributed.

The relative resemblance between the conformational populations in water and in the vacuum has been demonstrated repeatedly in the literature by experimental[15] or computational methods.[13,19] Thus, in water as in vacuum, the +gt and +g+g conformers are favored over the tt conformers.

The median angular velocity and median angular acceleration of the two dihedral angles are reported in Tables 5 and 6. Overall, velocities and accelerations are decreased in water relative to vacuum, but not by a constant factor. Indeed, the +g+g, +gt, −gt, and −g−g conformers are less affected than the t+g and tt conformers, where the breaking effect is around half. The effect is particularly strong for τ_3. Interestingly, the lesser affected t+g and tt conformers are also poorly populated ones.

Dynamic Behavior of Acetylcholine in Methanol. For additional insights, simulations were also run in methanol ($\epsilon =$ 33). The trajectory of τ_2 in methanol (Figure 9A) differs markedly from that in water (Figure 7A). Here, τ_2 is seen to residue only and equally in the two syn-clinal conformation +g and −g. Interconversion is via the syn-periplanar and never via anti-periplanar conformations. This may be due to solvent friction braking the rotation of the cationic headgroup, an effect that should be felt more strongly in the open geometries and is believed to account for the dynamic inaccessibility of $\tau_2 =$ trans.

The trajectory of τ_3 in methanol as in water fluctuates between 60° and 300° and mainly between 90° and 270° (Figure 9B). There is a clear preference for the anti-periplanar and anti-clinal geometries over the syn-clinal ones. Also, the latter have more open values than those found in water (90° and 270° rather than 60° and 300°), as if the bulky solvent would prevent a con-

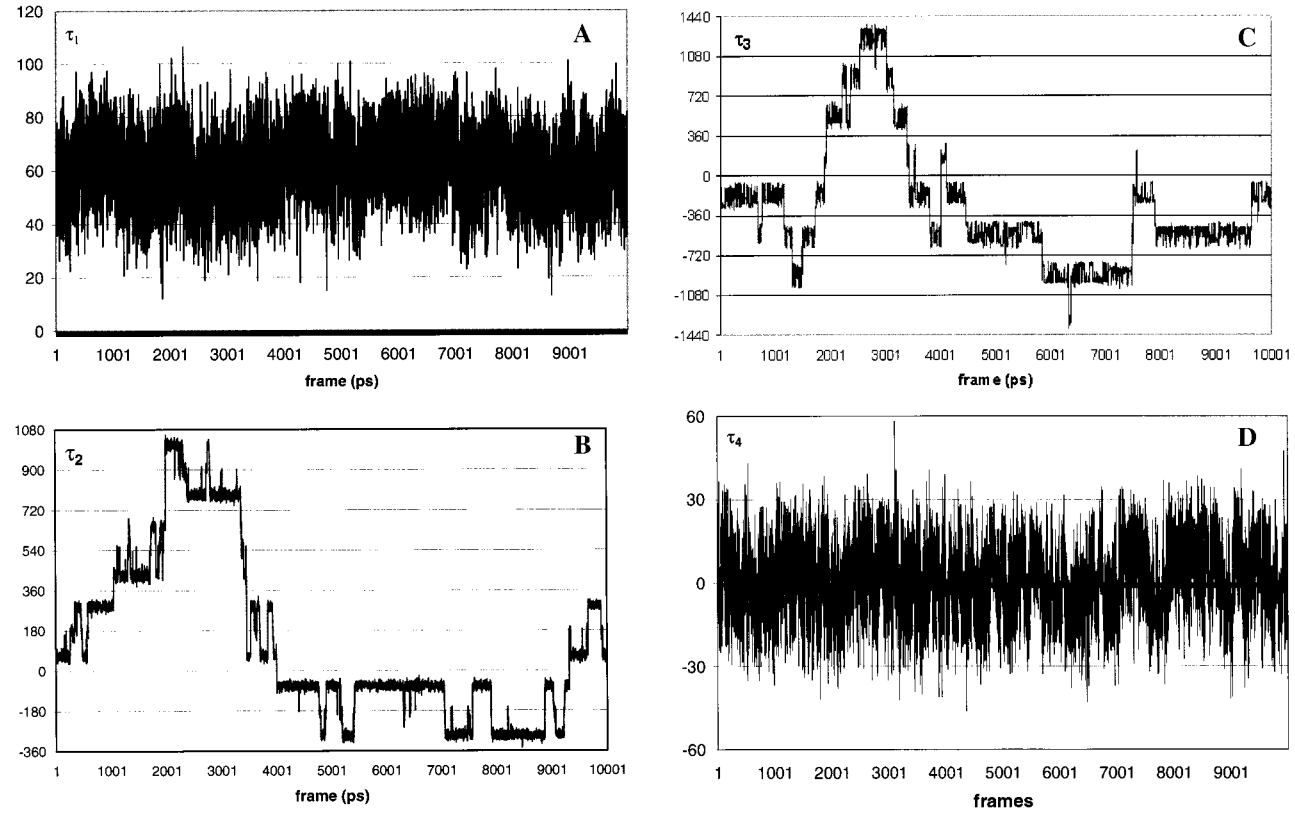

Figure 4. Variations of the dihedral angles τ_1 (A), τ_2 (B), τ_3 (C), and τ_4 (D) of acetylcholine in vacuum ($\epsilon = 1$; temperature, 300 K), as monitored during 10 ns.

Table 4. Number of Conformers in Each Class, As Accumulated during 5-ns Periods (Vacuum, $\epsilon = 1$)

conformations	0–5 ns	5–10 ns
+g+g	1945	1156
+gt	722	398
−g−g	1108	1996
−gt	431	740

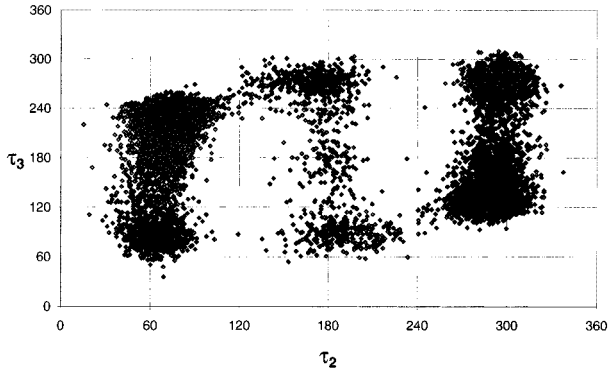

Figure 5. Conformational behavior of acetylcholine (τ_2 versus τ_3 plot) as simulated for 10 ns in vacuum with $\epsilon = 1$ at 300 K.

formational "closure". The predominance of the trans forms is ascribed to the polar and H-bond donor character of methanol, which will tend to favor conformations that maximize its access to the oxygen atoms.

When translated in terms of populations, the τ_2 versus τ_3 plot (Figure 10) reveals a marked symmetry between the four accessible conformations, namely, +g+g, +gt, −gt, and −g−g (Figure 10). The same symmetry is apparent in the median

Table 5. Median Angular Velocity (ω_M in deg/ps) and Median Angular Acceleration (α_M in deg/ps^2) of τ_2 in Acetylcholine, As Obtained by MD Simulations at 300 K in Vacuum with $\epsilon = 1$ and $\epsilon = 80$, in Water and in Methanol

	vacuum $\epsilon = 1$		vacuum $\epsilon = 80$		water		methanol	
conformers	ω_M	α_M	ω_M	α_M	ω_M	α_M	ω_M	α_M
+g+g	12.70	10.66	17.78	20.73	11.16	8.52	11.55	9.22
+gt	12.08	9.85	15.37	14.26	11.13	8.59	10.66	8.40
t+g	25.39	24.92	14.33	12.28	17.09	13.16		
tt	18.08	15.08	15.44	12.36	10.62	7.59		
t−g	24.23	24.06	13.53	10.35				
−gt	12.00	8.78	13.71	12.85	10.28	8.02	10.88	8.66
−g−g	12.21	8.96	12.10	10.99	9.75	7.78	11.41	9.12

Table 6. Median Angular Velocity (ω_M in deg/ps) and Median Angular Acceleration (α_M in deg/ps^2) of τ_3 in Acetylcholine, As Obtained by MD Simulations at 300 K in Vacuum with $\epsilon = 1$ and $\epsilon = 80$, in Water and in Methanol

	vacuum $\epsilon = 1$		vacuum $\epsilon = 80$		water		methanol	
conformers	ω_M	α_M	ω_M	α_M	ω_M	α_M	ω_M	α_M
+g+g	33.28	29.21	56.02	43.80	20.28	15.80	15.70	11.28
+gt	29.42	23.61	51.73	42.08	19.46	15.16	13.55	10.48
t+g	40.11	38.69	91.81	63.59	18.75	14.97		
tt	50.53	43.54	55.58	48.62	25.64	19.48		
t−g	39.52	38.84	82.91	59.94				
−gt	27.89	22.20	47.91	36.57	16.17	12.15	14.47	11.04
−g−g	32.56	27.91	51.03	38.96	18.16	13.73	15.00	11.34

angular velocities and median angular accelerations of τ_2 and τ_3 (Tables 5 and 6). Relative to water, the values of τ_2 have remained essentially unaffected, whereas the rotation of τ_3 is clearly slowed in methanol.

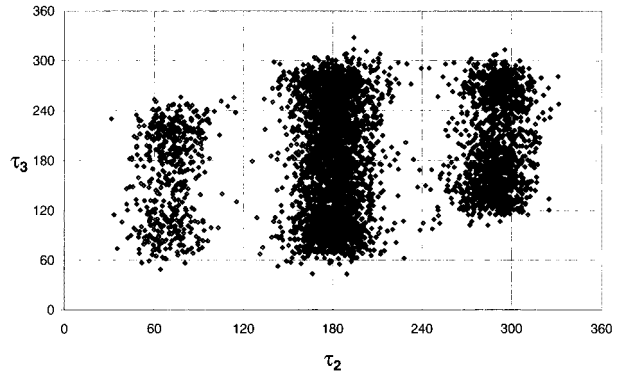

Figure 6. Conformational behavior of acetylcholine (τ_2 versus τ_3 plot) as simulated for 5 ns in vacuum with $\epsilon = 80$ at 300 K.

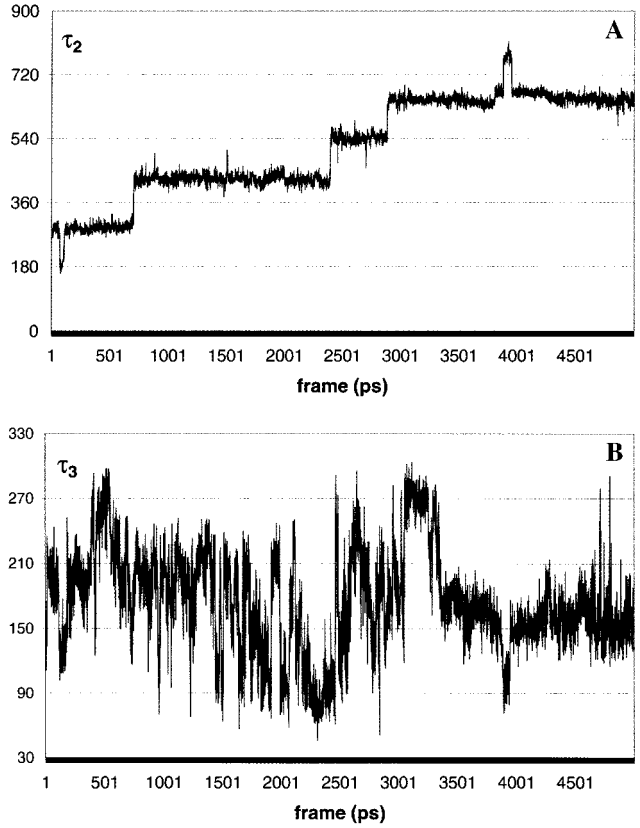

Figure 7. Variations of the dihedral angles τ_2 (A) and τ_3 (B) of acetylcholine in water at 300 K, as monitored during 5 ns.

Dynamic Behavior of Acetylcholine in 1-Octanol. Simulations were also run in hydrated octanol for 1.5 ns. As seen in Figure 11A, the angle τ_2 remains in the starting +g values (about 30°−100°) for the entire duration of the simulation. Clearly the friction of the bulky and viscous octanol on the rotation of the cationic headgroup is strong enough to completely prevent passage from +g to −g via $\tau_2 = 0°$, as well as via $\tau_2 = 180°$ as already noted in methanol. Had its starting geometry been −g, we can postulate that τ_2 would have remained in this angular quadrant.

The trajectory of τ_3 (Figure 11B) is restricted almost exclusively to anti-clinal conformations of the type −a (210°−260°) during the period from 0 to 1.4 ns, followed by a transition to an +a geometry. As under other conditions (see above), the angle τ_3 is more flexible than the angle τ_2. Had the simulation been conducted over a longer period, the values of τ_3 would

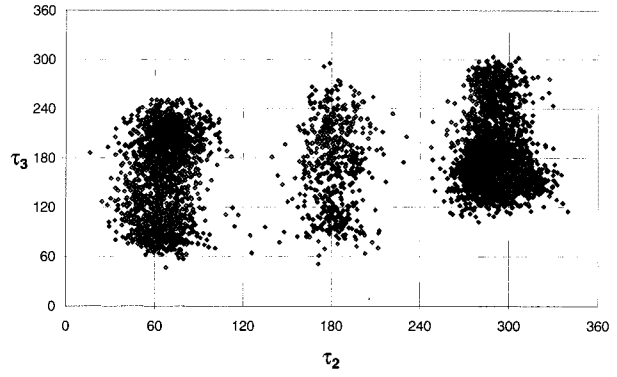

Figure 8. Conformational behavior of acetylcholine (τ_2 versus τ_3 plot) as simulated for 5 ns in water at 300 K.

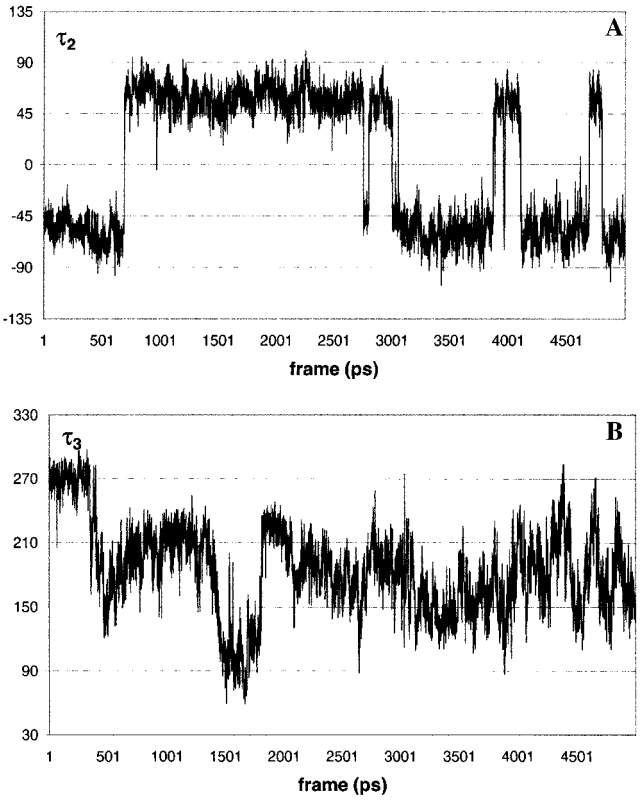

Figure 9. Variations of the dihedral angles τ_2 (A) and τ_3 (B) of acetylcholine in methanol at 300 K, as monitored during 5 ns.

presumably have been distributed more equally between −a and +a geometries.

The distribution of conformers shown on a τ_2 versus τ_3 plot (Figure 12) offers another representation of the very strong conformational constraints experienced by acetylcholine in octanol. This is due to the nonpolar character of the solvent, which induces folded conformers that maximize intramolecular interactions in the solute. The same phenomenon is also seen in the vacuum at low dielectric constant (Figure 5). In addition, there are two specific solvent effects revealed by the present simulations. First, solvent friction becomes a major factor in methanol and an overwhelming one in octanol. Second, because acetylcholine and octanol have a comparable molecular size, they will tend to adapt comparable shapes to favor steric fit. The usual conformational calculations in the vacuum obviously fail to take such factors into account, which limits the biological relevance of their results.

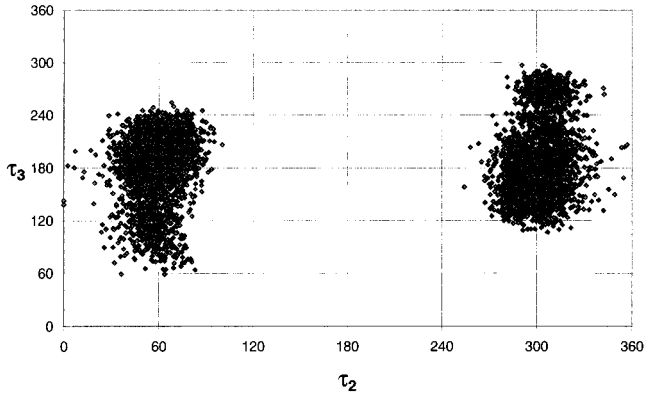

Figure 10. Conformational behavior of acetylcholine (τ_2 versus τ_3 plot) as simulated for 5 ns in methanol at 300 K.

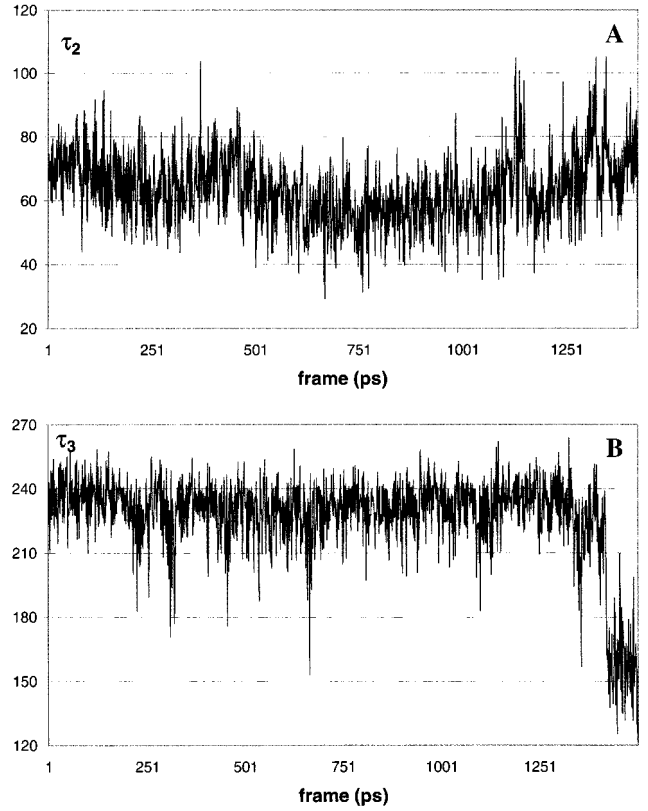

Figure 11. Variations of the dihedral angles τ_2 (A) and τ_3 (B) of acetylcholine in 1-octanol at 300 K, as monitored during 1.5 ns.

The median angular velocities and median angular accelerations of τ_2 and τ_3 in octanol (Table 7) reveal further constraints. But because the conformational is now so restricted, direct comparison with behavior under other conditions is difficult.

Average Angular Velocity and Angular Acceleration of Acetylcholine under Different Conditions. The data compiled in Tables 5−7 allow a superficial comparison of the solvent influence on the median angular velocities and median angular accelerations of τ_2 and τ_3 in acetylcholine. However, and as stated above, the difference in conformer populations limits the scope of such a comparison. To gain more insight, the median velocities and median accelerations of τ_2 and τ_3 were averaged for all transitions and for all frames observed in a given solvent. The results (Table 8) reveal a number of facts. First, the velocities and accelerations are seen to vary considerably over an entire simulation, since the standard deviations have very

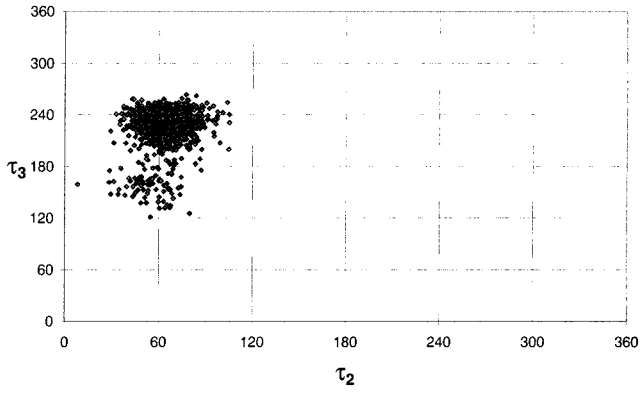

Figure 12. Conformational behavior of acetylcholine (τ_2 versus τ_3 plot) as simulated for 1.5 ns in 1-octanol at 300 K.

Table 7. Median Angular Velocity (ω_M in deg/ps) and Median Angular Acceleration (α_M in deg/ps^2) of τ_2 and τ_3 in Acetylcholine, as Obtained by MD Simulations in Hydrated Octanol at 300 K

	τ_2		τ_3	
conformers	ω_M	α_M	ω_M	α_M
+g+a	12.22	11.50	21.35	19.01
+gt	9.82	7.19	20.24	15.44
+g−a	9.45	7.07	11.54	8.09

Table 8. Average Angular Velocity (ω_M in deg/ps ± SD) and Average Angular Acceleration (α_M in deg/ps^2 ± SD) of τ_2 and τ_3 in Acetylcholine, As Obtained by MD Simulations under Different Solvent Conditions at 300 K[a]

solvent conditions	τ_2		τ_3	
	ω_M	α_M	ω_M	α_M
vacuum $\epsilon = 1$	16.6 ± 15.3 (±0.3)	12.1 ± 15.3 (±0.3)	31.8 ± 35.5 (±0.7)	26.5 ± 33.8 (±0.7)
water	11.0 ± 9.1 (±0.3)	9.4 ± 7.8 (±0.3)	18.5 ± 16.3 (±0.5)	14.1 ± 13.6 (±0.4)
methanol	10.6 ± 9.2 (±0.3)	8.3 ± 8.0 (±0.2)	14.4 ± 11.8 (±0.3)	11.0 ± 9,8 (±0.3)
octanol	9.8 ± 7.8 (± 0.4)	7.3 ± 6.2 (±0.3)	12.6 ± 10.1 (±0.5)	9.1 ± 8.2 (±0.4)

[a] The 95% confidence limits (95%CL) are reported in parentheses after the SD.

broad values. These reflect the great flexibility of acetylcholine and the broad range of velocities and accelerations its dihedral angles can span during the simulations. Second, τ_3 clearly shows a greater flexibility than τ_2, particularly in the vacuum where the velocity and acceleration of the former are about twice those of the latter.

Third, and more importantly, Table 8 demonstrates quantitatively how an increasing molecular size of the solvent slows down internal rotations in acetylcholine. The 95% confidence limits of ω_M and α_M (reported in parentheses in Table 8) were calculated from the SD for 10 000, 5000, or 1500 frames depending on the solvent. The 95% CL demonstrate that the differences in velocities and accelerations between solvents are highly significant in statistical terms. The effect cannot be ascribed to medium polarity per se, since this would yield comparable values for octanol and the vacuum at $\epsilon = 1$. What is thus observed is a marked decline in velocity and acceleration when going from vacuum to water and a further but lesser decline in methanol and then in octanol. These effects are less marked and less diversified for τ_2 than for τ_3, probably because

the braking of the rotation of the cationic headgroup is less sensitive to solvent size.

Discussion

Conformational Preferences. The prime objective of this work was not to investigate solvent influences on conformation preferences. Nevertheless, a comparison with published data appears of interest. Thus, a conformational study of acetylcholine in D_2O showed a predominance of the tg form.[6] X-ray crystallographic investigations yielded more complex results, since the conformer frozen in crystals depends to a large extent on the counterion, e.g., gg for the bromide and tg for the chloride.[22] Recent ab initio studies have refined previous investigations, indicating a preference for the tg conformer.[16] The tt conformer has been shown to be recognized by acetylcholinesterase[5] and the muscarinic receptors, whereas the tg conformer interacts with the nicotinic receptors.[14] Also, bidimensional NMR studies have shown that when acetylcholine interacts with the nicotinic receptor, its cationic head undergoes a conversion from an extended tt to a folded tg conformation.[18]

In our study, the tt conformations never predominated in any of the simulations, being present in low proportions in vacuum at $\epsilon = 1$ and in water and absent in methanol and octanol. The only simulation that revealed a marked proportion of tt conformers was in the vacuum at $\epsilon = 80$. This may be explained by the fact that media of high polarity weaken the intramolecular electrostatic interactions that stabilize the folded conformers. Furthermore, any solvent whatever its polarity will tend to favor folded conformers since these will minimize friction with the solvent, as noted above. In other words, the lower the polarity of the medium, the higher the proportion of folded conformers, an effect reinforced by the mere presence of a solvent (compared to the vacuum). In a biological perspective, it is of course worth noting that the tt conformers which predominate in vacuum at $\epsilon = 80$ are those recognized by the muscarinic receptors. A priori, a vacuum at $\epsilon = 80$ would appear as a nonrealistic environment, but perhaps the muscarinic binding site does resemble a solvent-free cavity with a high polarity resulting from polar residues.

Solvent Constraints on Conformational Dynamics. Much more than the conformational preferences of acetylcholine taken as a representative compound, the major objective of this work was to assess the influence of solvents on its molecular motions. By simulating the behavior of acetylcholine in vacuum and in solvents of increasing molecular weight (water, methanol, octanol), this work has demonstrated a progressive loss of conformational freedom. In line with our primary objective, the median angular velocity (ω_M) and the median angular acceleration (α_M) of the dihedral angles τ_2 and τ_3 were also found to decrease markedly in the series vacuum ($\epsilon = 1$) > water > methanol > octanol, with a total decrease of about 40% and 60% for the average values of τ_2 and τ_3, respectively.

As demonstrated here, the influence of solvent on a solute's internal motions is quantifiable and significant. These results add a new dimension to our understanding of the interactions between a compound and its molecular environment.[1−3] Furthermore, they invite speculation on the biological and pharmacological relevance of such medium-dependent constraints.

Messenger molecules, drugs, and toxins must often penetrate into or cross highly organized biological media (membranes, microtubules, etc.) before reaching their targets (receptors, enzymes, nucleic acids, etc.). The present results indicate that the flexibility of biomolecules will be markedly reduced while they interact with such biological media. The intensity of this phenomenon cannot be calculated from the present results, but the trend apparent in the sequence vacuum < water < methanol < octanol would suggest that membranes might cause a dramatic slowing down of intramolecular motions in permeants. The computational capacities now available render this hypothesis testable.

Assuming this hypothesis is verified, what would its implications be in terms of binding to receptors or enzymes? A priori, such "freezing" may constrain a biomolecule either in a conformation recognized by the binding site (active conformation) or in an inactive one. In turn, this picture suggests a mechanism of membrane-mediated selectivity that acts as a preliminary filter by either favoring receptor binding or rendering it more difficult. But whatever the ultimate veracity of such a hypothesis, it suggests that the dynamic dimensions of molecule−medium interactions may be a fertile ground for future investigations.

JA0119999

(22) Caillet, J.; Claverie, P.; Pullman, B. *Acta Crystallogr. B* **1978**, *B34*, 3266−3272.
(23) Testa, B.; Carrupt, P. A.; Gaillard, P.; Billois, F.; Weber, P. *Pharm. Res.* **1996**, *13*, 335−343.
(24) Carrupt, P. A.; Testa, B.; Gaillard, P. Computational approaches to lipophilicity: Methods and applications. In *Reviews in Computational Chemistry*; Lipkowitz, K. B., Boyd, D. B., Eds.; Wiley-VCH: New York, 1997; Vol. 11, pp 241−315.
(25) Pagliara, A.; Carrupt, P. A.; Caron, G.; Gaillard, P.; Testa, B. *Chem. Rev.* **1997**, *97*, 3385−3400.
(26) Pagliara, A.; Testa, B.; Carrupt, P. A.; Jolliet, P.; Morin, Ch.; Morin, D.; Urien, S.; Tillement, J. P.; Rihoux, J. P. *J. Med. Chem.* **1998**, *41*, 853−863.